First-principles study and electronic structures of Mn-doped ultrathin ZnO nanofilms

E. Salmani[a)], A. Benyoussef[a)], H. Ez-Zahraouy[a)†], E. H. Saidi[b)], and O. Mounkachi[c)]

[a)] *LMPHE (URAC 12), Departement de Physique, Faculté des Sciences, Université Mohammed V-Agdal, Rabat, Morocco*

[b)] *LPHE, Departement de Physique, Faculté des Sciences, Université Mohammed V-Agdal, Rabat, Morocco*

[c)] *Institute of Nanomaterials and Nanotechnology, MAScIR, Rabat, Morocco*

(Received 29 January 2012; revised manuscript received 3 April 2012)

The first-principles density functional calculation is used to investigate the electronic structures and magnetic properties of Mn-doped and N-co-doped ZnO nanofilms. The band structure calculation shows that the band gaps of ZnO films with 2, 4, and 6 layers are larger than the band gap of the bulk with wurtzite structure and decrease with the increase of film thickness. However, the four-layer ZnO nanofilms exhibit ferromagnetic phases for Mn concentrations less than 24% and 12% for Mn-doping performed in the whole layers and two layers of the film respectively, while they exhibit spin glass phases for higher Mn concentrations. It is also found, on the one hand, that the spin glass phase turns into the ferromagnetic one, with the substitution of nitrogen atoms for oxygen atoms, for nitrogen concentrations higher than 16% and 5% for Mn-doping performed in the whole layers and two layers of the film respectively. On the other hand, the spin-glass state is more stable for ZnO bulk containing 5% of Mn impurities, while the ferromagnetic phase is stable by introducing the p-type carriers into the bulk system. Moreover, it is shown that using the effective field theory for ferromagnetic system, the Curie temperature is close to the room temperature for the undamped Ruderman–Kittel–Kasuya–Yoshida (RKKY) interaction.

Keywords: ultra thin film, ZnO, *ab initio*, electronic structure, magnetic properties, effective field theory

PACS: 66.30.Xj, 72.20.Dp, 72.20.My, 72.25.Dc **DOI:** 10.1088/1674-1056/21/10/106601

1. Introduction

Zinc oxide (ZnO), which is a II–VI semiconductor compound, is stable in the wurtzite structure and has a wide band gap of 3.4 eV. It has attracted intensive research efforts for its unique properties and versatile applications in transparent electronics, ultraviolet (UV) light emitters, piezoelectric devices, chemical sensors, and spin electronics.[1−10] Transparent thin film transistors (TFTs) with ZnO used as an active channel have achieved much higher field effect mobility than amorphous silicon TFTs.[11−13] These transistors can be widely used for display equipment. ZnO has been proposed to be a more promising UV emitting phosphor than GaN because of its larger exciton binding energy (60 meV). This leads to a reduced UV lasing threshold, thereby yielding a higher UV emitting efficiency at room temperature.[14] Surface acoustic wave filters using ZnO films have already been used for video and radio frequency circuits. Piezoelectric ZnO thin film has been fabricated into ultrasonic transducer arrays operating at 100 MHz.[15] Bulk and thin films of ZnO each have demonstrated to possess a high sensitivity to toxic gases.[16−19] Furthermore, hole mediated ferromagnetic ordering in bulk ZnO by introducing Mn as dopant has been predicted theoretically[20] and reported experimentally.[21] The calculations of the piezoelectricity in ZnO nanofilms show that the effective piezoelectric constant increases with film thickness increasing.[22] The dependences of electronic structure and magnetic property on film thickness remain unknown. What is more, for ultrathin ZnO nanofilms, quantum effects might have a remarkable influence on their properties. Up to date, there has been no work dedicated to investigating them yet. The purpose of this paper is to study, by using first-principles calculations, the electronic structures and magnetic properties of Mn-doped and N-co-doped ZnO nanofilms in both cases, totally doping (the doping is performed homogeneously in the whole layers of the film) and partially doping (the doping is performed only on a few layers of the film). The ef-

†Corresponding author. E-mail: ezahamid@fsr.ac.ma

© 2012 Chinese Physical Society and IOP Publishing Ltd

fects of the film thickness on band gap structure and stability of the ferromagnetism are also investigated.

2. Model and calculation method

The band structure of wurtzite $Zn_{1-x}Mn_xO$ is calculated using the Korringa–Kohn–Rostoker method combined with the coherent potential approximation (KKR–CPA), with the parameterization of Moruzzi, Janak and Williams (MJW) and Vosko, Wilk and Nusair (VWN).[23] A fraction of Zn atoms are replaced by magnetic impurities randomly. The KKR–CPA is one of the most sophisticated methods to treat such substitutional disordered systems by taking disorder into account in an *ab initio* manner. Akai and Dederichs have developed the KKR–CPA method to treat transition metal alloys[24] and InAs-based DMS,[25] and explained their magnetic properties successfully. The form of the crystal potential is approximated by a muffin-tin potential, and the wave functions in the respective muffin-tin spheres are expanded in real harmonics up to $l = 2$, where l is the angular momentum quantum number defined at each site. We use higher K-points up to 250 in the irreducible part of the first Brillouin zone (for all details see Ref. [26]). In the present calculations, we use the KKR-CPA code MACHIKANEYAMA2002v09 package.[27]

The optimized structures are obtained by calculating the total energy of ZnO as a function of the lattice constant. It is found that the lattice constant increases with thickness of the film increasing (Fig. 1).

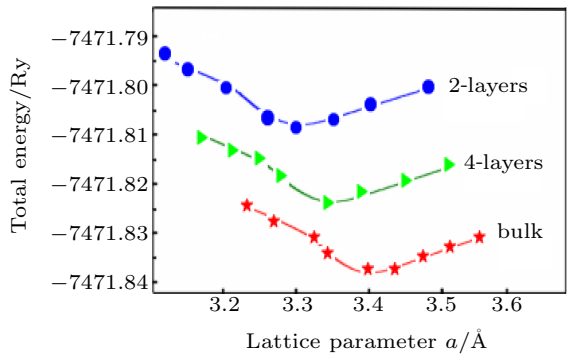


Fig. 1. (color online) First-principles results showing the total energy versus lattice parameter (1 Å=0.1 nm), where minimal values of energy–lattice curves each indicate a decrease in lattice constant.

On the other hand, we study the carrier-mediated exchange interaction, the so-called Ruderman–Kittel–Kasuya–Yoshida (RKKY) coupling; between two magnetic impurity moments in p-type Mn-doped ZnO using effective field theory. We extract both the short and long impurity–impurity distance behaviors. One of the most important properties of magnetic impurities in DMS is the effective interaction between them propagated by the holes or electrons in the bulk host, the so-called Ruderman–Kittel–Kasuya–Yoshida (RKKY) coupling.[28−33] Several models have been proposed to explain the nature of the exchange interaction in DMS; double exchange, bound magnetic polaron, and Ruderman–Kittel–Kasuya–Yosida (RKKY) interaction. The *ab initio* calculation of doped ZnO with defects shows that a dominant interaction is RKKY.[34,35] This coupling is crucial for magnetic ordering of the impurities, but also offers access to the intrinsic magnetic properties of the host. In a previous work on the RKKY coupling in DMS,[36,37] using the effective field theory, with a Honmura–Kaneyoshi differential operator technique, the transition temperature has been obtained for ferromagnetic Mn-doped ZnO diluted magnetic semiconductor, the RKKY coupling has then been calculated from the electronic strucrture calculation. There are two kinds of RKKY interaction, damped and undamped to simulate magnetic coupling; we use the damped RKKY interaction when the carries (holes or electrons) each have a high kinetic energy and the undamped RKKY interaction when the carries each have a low kinetic energy to stabilize ferromagnetic interaction.[37] The Hamiltonian we use contains a damped and undamped RKKY interaction model to describe the exchange coupling constants J_{ij} between the local moments M_{ni} and M_{nj}. We consider a diluted Ising spin ferromagnetic system consisting of spin 5/2 on a wurtzite lattice, corresponding to the ZnO structure. The Hamiltonian of our system takes the form of

$$H = -\sum_{i,j} J^{\mathrm{RKKKY}}(r_{ij})(n_i n_j S_i^Z S_j^Z),$$

where n_i is the occupation number of the magnetic impurity and $J^{\mathrm{RKKR}}(r_{ij})$ is the RKKY range function which takes the form of

$$J^{\mathrm{RKKY}}(r) = J_0\, \mathrm{e}^{-r/l} r^{-4} \times \left[\sin(2K_{\mathrm{F}}r) - 2K_{\mathrm{F}}r\cos(2K_{\mathrm{F}}r)\right].$$

We take higher value of l (undamped RKKY interaction) for long-range RKKY coupling, and small value of l (damped RKKY interaction) for short-range RKKY coupling. From the band structure calculation,

we derive the band splitting Δ and the values of exchange constant $N_0\beta$ for different values of impurity concentration $n_{\rm i}$ and hole concentration $n_{\rm c}$. In the formula given above, $K_{\rm F} = \left(\frac{3}{2}\pi^2 n_{\rm c}\right)^{1/3}$ is the Fermi wave number, and r_{ij} is the separation between moments in the sites i and j. The magnetic coupling $J_0 > 0$ is related to the local zener coupling $J_{\rm pd}$ between the Mn local moment and the hole spin, and S_i^z is a spin random variable of site i which takes the values $\pm 1/2$, $\pm 3/2$, $\pm 5/2$. With DMS materials being at best poor metals, we also introduce into the RKKY range function a damping factor $\mathrm{e}^{-r/l}$ where the damping scale l is related to the carrier mean free path or perhaps a carrier localization length arising from Anderson localization of the free carriers, however, we use $l = a$ (the distance between first nearest neighbours) in order to study the short-range RKKY coupling, and for long-ranged RKKY we use $l = b$ (the distance between second nearest neighbours). Our goal here is to obtain explicitly the ideal RKKY phase diagram, and to clarify the physical background for the characteristic behaviors of ($T_{\rm c}$, $n_{\rm c}$) observed in the diluted spin-S Ising ferromagnetic system. The method is detailed in Ref. [37] in which a Mn-doped ZnO wurtzite structure is studied using the effective field theory.

3. Results and discussion

The band structures of ZnO bulk and nanofilms of 2 and 4 layers have been computed. Figures 2(a) and 2(b) show that the ZnO film is semiconductive and has direct band gaps at the Γ point, similar to wurzite bulk ZnO shown in Fig. 2(c).

The band gaps of ZnO films of 2 and 4 layers are larger than the gap of the bulk with a wurtzite structure. The gap decreases with the increase of the thickness of film, and will reach 0.10 Ry (1 Ry=13.605 eV) of wurtzite ZnO bulk for sufficiently large film thickness as shown in Fig. 3. This may be attributed to the fact that with the growth of the film thickness, the electrons in the film are less confined. As a result, the confinement effects in the film become weaker, leading to the decrease of the band gap.

Joseph *et al.*[38] prepared p-type ZnO thin films successfully by using the co-doping method. Indeed, this result can be confirmed if the hole mediated ferromagnetism is the dominant mechanism, and the attainment of p-type ZnO can pave the way for a promising potential of Mn-doped ZnO. Therefore, it is worth investigating the carrier-induced ferromagnetism in the ZnO-based DMS. The various experimental and theoretical investigations of the magnetic order in $Zn_{1-x}Mn_xO$ give discrepant results.

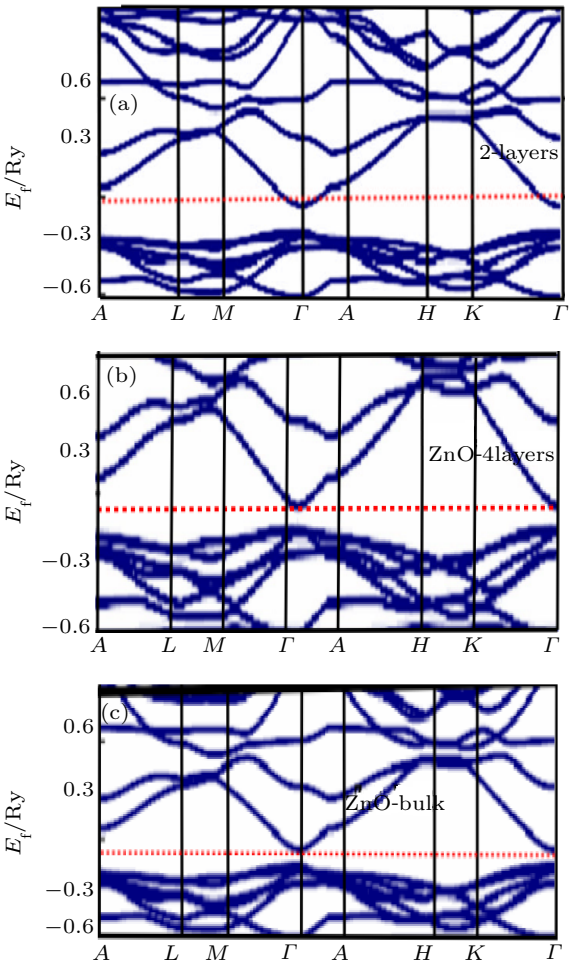


Fig. 2. (color online) Band structure calculations of two-layer ZnO nanofilms (a), four-layer ZnO nanofilms (b), and ZnO bulk (c).

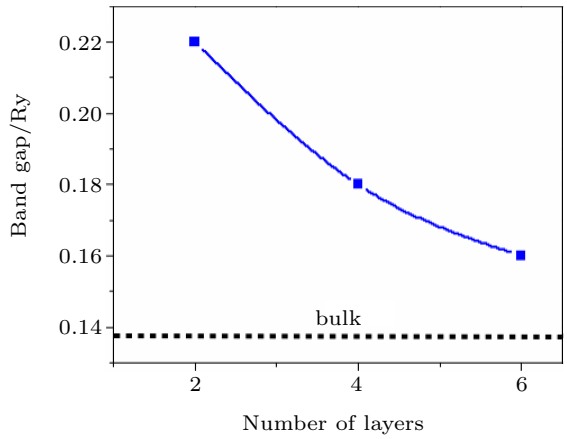


Fig. 3. (color online) Variation in the band gap of ZnO with number of layers coped with ZnO bulk.

However, Sharma *et al.*[39] have reported on the ferromagnetism in (Zn,Mn)O systems, while others Tiwari *et al.*[40] observed spin-glass behavior. An experimental study finds no evidence for magnetic order, down to $T = 2$ K.[41] These conflicting results also exist concerning the distribution of Mn in ZnO. From the experimental results given by Cheng *et al.*[42] we are aware that Mn is distributed homogeneously. Yet Jin *et al.*[43] reported on the clustering of Mn atoms. Sato and Katayama-Yoshida[44] carried out the KKR–CPA calculation in randomly substituted 3d TM impurities in ZnO and found the ferromagnetic state (FM) to be stable for half-filled or more than half-filled impurities such as V, Cr, Fe, Co, and Ni, while a spin-glass-like state is found to be stable for ZnO containing 5% of Mn impurities. Mn impurities are introduced randomly into cation sites of the ZnO semiconductor. This disordered substitution in a diluted magnetic semiconductor (DMS) is well described by the Korringa–Kohn–Rostoker coherent-potential approximate (KKR–CPA) method. With respect to previous theoretical studies, $Zn_{1-x}Mn_xO$ is not ferromagnetic in the absence of additional carriers. In order to stabilize the FM phase, it is necessary to insert carriers into the system. Our calculation (Table 1, Fig. 4), in the case of Mn-doped ZnO bulk, confirms on the one hand the stability of the spin-glass state found by Sato and Katayama–Yoshida[34] and, on the other hand, the stability of the ferromagnetic state by introducing the p-type carriers into the bulk system, which is consistent with the result in Ref. [45]. In the case of ZnO nanofilms, it is clear from Table 2 that the ferromagnetic phase is stable for Mn concentrations less than 24% and 12% for Mn-doping performed in the whole layers (1111) (see Fig. 5 and Fig. 6) and two layers (1100) (see Fig. 7 and Fig. 8) of the film, respectively. While it exhibits a spin-glass phase for higher Mn concentrations, which is well accordant with the results obtained in Ref. [38]. In addition, the spin-glass phase turns into a ferromagnetic one, with the substitution of nitrogen atoms for oxygen atoms, for nitrogen concentrations higher than 5% (see Fig. 9) and 16% (see Fig. 10) for Mn-doping performed in the whole layers and two layers of the film, respectively.

Moreover, for Mn-doped ZnO nanaofilm with 16% of hole concentration, the Curie temperature is smaller than that for the bulk one, which is in good consistence with the experimental result obtained in Ref. [45]. We note that in the case of four layers, the vacancy sites are not responsible for the half metallic behavior as shown in Fig. 11, in contrast to the case of ZnO bulk.[34]

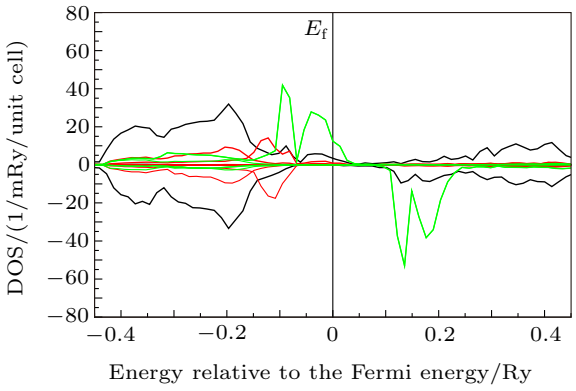


Fig. 4. (color online) Total, d, and p states projected density of states (DOS) $Zn_{1-x}Mn_xO_{1-y}N_y$ bulk, with $x = 0.05$ and $y = 0.04$. The total DOS is denoted by a solid black line, 3d-states of Zn by solid green line, 2p-states of O, and N by a solid red line.

Table 1. Total energy differences between ferromagnetism and antiferromagnetism in the case of $Zn_{1-x}Mn_xO_{1-y}N_y$ bulk, with $x = 0.05$ and $y = 0.01$; 0.02; 0.03; $y = 0.04$ within the standard LDA.

Compound (ZnO bulk)	$(E_{\text{spin-glass}} - E_{\text{FM}})$/Ry
$Zn_{0.95}Mn_{0.05}O$	-1.196×10^{-4}
$Zn_{0.95}Mn_{0.05}O_{0.99}N_{0.01}$	-1.164×10^{-4}
$Zn_{0.95}Mn_{0.05}O_{0.98}N_{0.02}$	-7.3×10^{-5}
$Zn_{0.95}Mn_{0.05}O_{0.97}N_{0.03}$	-1.653×10^{-5}
$Zn_{0.95}Mn_{0.05}O_{0.96}N_{0.04}$	2.4×10^{-5}

Table 2. Total energy differences between ferromagnetic and spin- glass state in the case of four-layer ZnO nanofilms doped with Mn and/or co-doped Mn and N within the standard LDA.

Compound (ultrathin ZnO nanofilms four layers)	$(E_{\text{spin-glass}} - E_{\text{FM}})$/Ry
Four-layer $Zn_{0.95}Mn_{0.05}O$ with configuration 1100	7.959×10^{-4}
Four-layer $Zn_{0.88}Mn_{0.12}O$ with configuration 1100	-1.354×10^{-4}
Four-layer $Zn_{0.76}Mn_{0.24}O$ with configuration 1100	-1.0155×10^{-3}
Four-layer $Zn_{0.88}Mn_{0.12}O_{0.95}N_{0.05}$ with configuration 1100	8.3536×10^{-3}
Four-layer $Zn_{0.95}Mn_{0.05}O$ with configuration 1111	1.341×10^{-4}
Four-layer $Zn_{0.88}Mn_{0.12}O$ with configuration 1111	7.042×10^{-4}
Four-layer $Zn_{0.76}Mn_{0.24}O$ with configuration 1111	-4.88×10^{-5}
Four-layer $Zn_{0.76}Mn_{0.24}O_{0.88}N_{0.16}$ with configuration 1111	9.39×10^{-5}

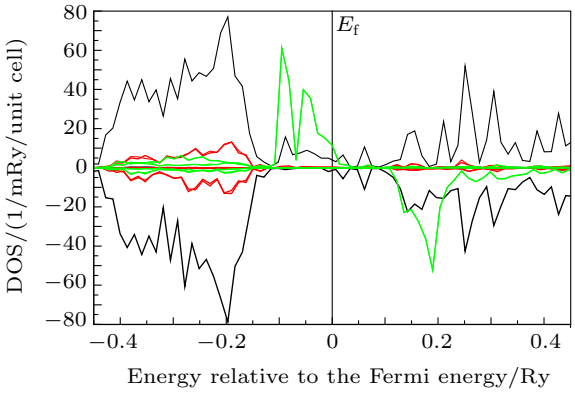


Fig. 5. (color online) Total, d, and p states projected density of state (DOS) of nanofilm four-layer configuration (1100) $Zn_{1-x}Mn_xO$, with $x = 0.05$, the total DOS is denoted by a solid black line, 3d-state of Zn by solid green line, and 2p-states of O by a solid red line.

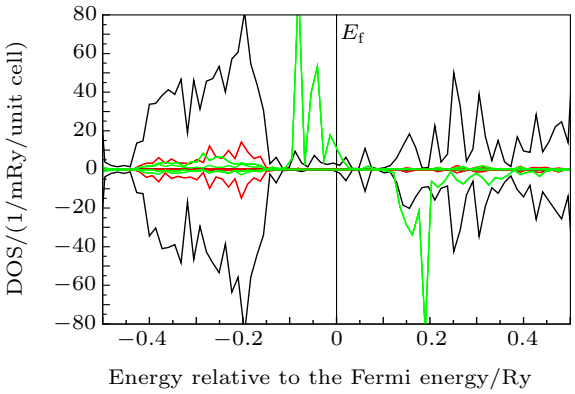


Fig. 6. (color online) Total, d, and p states projected density of state (DOS) nanofilm four-layer configuration (1111) $Zn_{1-x}Mn_xO$, with $x = 0.05$. The total DOS is denoted by a solid black line, 3d-state of Zn by solid green line, 2p-states of O by a solid red line.

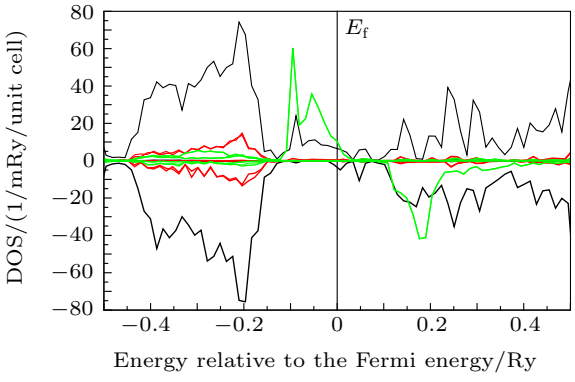


Fig. 7. (color online) Total, d, and p states projected density of state (DOS) of four-layer configuration (1100) $Zn_{1-x}Mn_xO$ nanofilms, with $x = 0.12$. The total DOS is denoted by a solid black line, 3d-state of Zn by solid green line, and 2p-states of O by a solid red line.

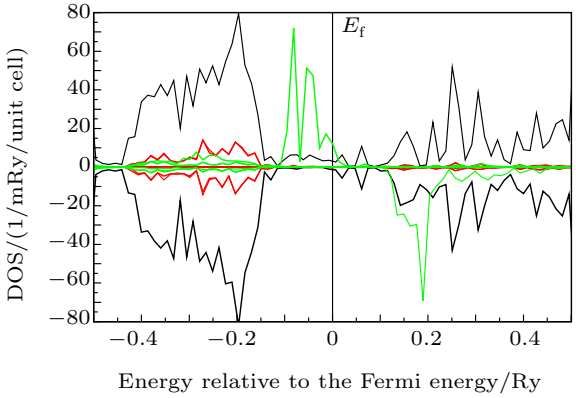


Fig. 8. (color online) Total, d, and p states projected density of state (DOS) of four-layer configuration (1100) $Zn_{1-x}Mn_xO_{1-y}N_y$, with $x = 0.12$ and $y = 0.05$. The total DOS is denoted by a solid black line, 3d-states of Zn by solid green line, and 2p-states of O and N by a solid red line.

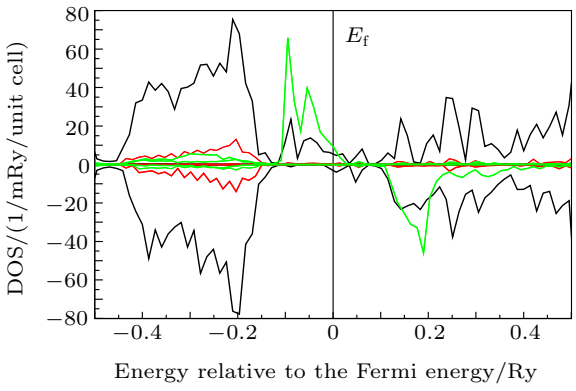


Fig. 9. (color online) Total, d, and p states projected density of state (DOS) of four-layer configuration (1111) $Zn_{1-x}\mathbf{Mn}_xO$ nanofilms, with $x = 0.24$. The total DOS is denoted by a solid black line, 3d-states of Zn by solid green line, and 2p-states of O by a solid red line.

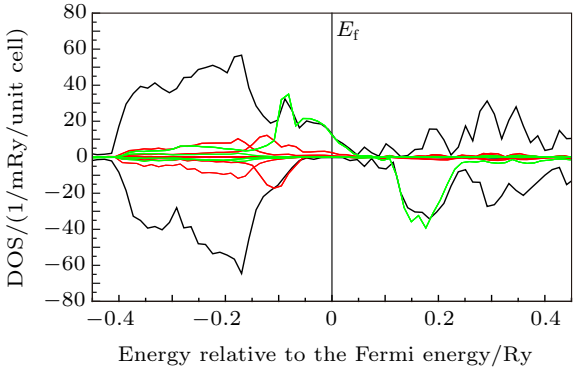


Fig. 10. (color online) Total, d, and p states projected density of state (DOS) of four-layer (1111) $Zn_{1-x}Mn_xO_{1-y}N_y$ nanofilms, with $x = 0.24$ and $y = 0.16$. The total DOS is denoted by a solid black line, 3d-states of Zn by solid green line, and 2p-states of O and N by a solid red line.

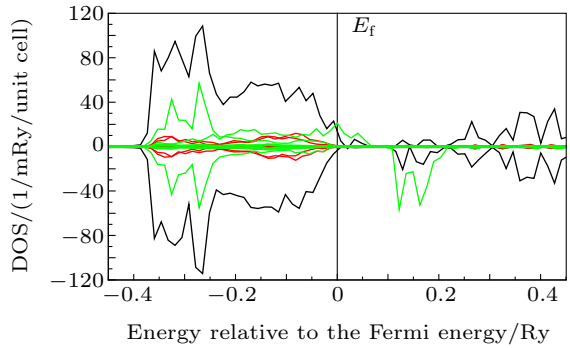


Fig. 11. (color online) Total, d, and p states projected density of state (DOS) of four-layer configuration (1111) $Zn_{1-x-y}Mn_xVc_yO$ nanofilms, with $x = 0.06$ and $y = 0.06$. The total DOS is denoted by a solid black line, 3d-states of Zn by solid green line, and 2p-states of O by a solid red line.

Furthermore, the effect of temperature on the magnetic property of Mn-doped ZnO nanofilm is studied by using effective field theory with an RKKY interaction model. For $Zn_{1-x}Mn_xO_{1-y}N_y$ ($x = 0.24$ and $y = 0.16$) holes are itinerant with keeping their d-characteristic due to the large hybridization of the N-p state with the Mn-3d state (Fig. 10). In the case of $Zn_{1-x}Mn_xO_{1-y}N_y$ ($x = 0.24$ and $y = 0.16$) the doped holes go with the Mn-3d states into VBM at E_f level, holes are more itinerant so their kinetic energies are higher and the ferromagnetic state is probably stabilized by the RKKY d–d exchange mechanism. We use two types of d–d RKKY interactions (damped and undamped) to simulate Curie temperatures for these samples and to approach to experimental value $T_c = 290$ K.[45]

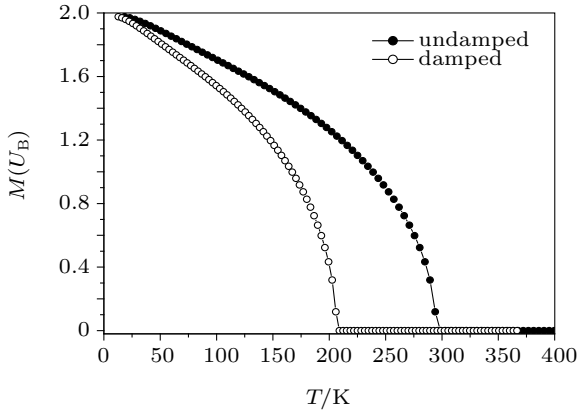


Fig. 12. The behaviors of magnetization M as a function of temperature for $Zn_{1-x}Mn_xO_{1-y}N_y$, in the case of four-layer nanofilm (1111) with $x = 0.24$ and $y = 0.16$ for damped and undamped RKKY interaction.

The behavior of the magnetization as a function of temperature is presented in Fig. 12, for $Zn_{1-x}Mn_xO_{1-y}N_y$ ($x = 0.24$ and $y = 0.16$) in the case of totally Mn-doping four layers (1111) with damped and undamped RKKY interaction. It is found that in the case of damped RKKY interaction, the Curie temperature is less than room temperature, while, in the undamped RKKY interaction case it is close to the room temperature. This is due to the fact that the holes are more itinerant so their kinetic energies are higher and then they mediate ferromagnetism.

4. Conclusion

On the basis of first-principles density functional calculations, we studied the electronic and magnetic properties of Mn-doped and M–N-doped ultrathin ZnO nanofilms. It is found that the band gap of ZnO film is larger than that of the bulk with a wurtzite structure and decreases with film thickness increasing. We also show that the stability of the spin glass and the ferromagnetic states depend strongly on how Mn-doping is carried out. Indeed, we show that the four-layer ZnO nanofilm exhibits a ferromagnetic phase for Mn concentrations less than 24% and 12% for Mn-doping performed in the whole layers and two layers of the film, respectively, while it exhibits spin-glass phase for higher Mn concentrations.

Acknowledgment

We thank professor Hisazumi Akai for fruitful discussion and for providing us with his KKR–CPA band structure calculation package (MACHIKANEYAMA-2000). LMPHE"Unité de Recherche Associée au CNRST (URAC)"

References

[1] Nomura K, Ohta H, Ueda K, Kamiya T, Hirano M and Hosono H 2003 *Science* **300** 1269
[2] Nakada T, Hirabayashi Y, Tokado T, Ohmori D and Mise T 2004 *Sol. Energy* **77** 739
[3] Lee S Y, Shim E S, Kang H S, Pang S S and Kang J S 2005 *Thin Solid Films* **437** 31
[4] Könenkamp R, Word R C and Schlegel C 2004 *Appl. Phys. Lett.* **85** 6004
[5] Mckinstry S T and Muralt P 2004 *J. Electroceram.* **12** 7
[6] Wang Z L, Kong X Y, Ding Y, Gao P, Hughes W L, Yang R and Zhang Y 2004 *Adv. Funct. Mater.* **14** 943
[7] Wagh M S, Patil L A, Seth T and Amalnerkar D P 2004 *Mater. Chem. Phys.* **84** 228

[8] Ushio Y, Miyayama M and Yanagida H 1994 *Sensor Actuator* B **17** 221
[9] Harima H 2004 *J. Phys.: Condens. Matter* **16** S5653
[10] Pearton S J, Heo W H, Ivill M, Norton D P and Steiner T 2004 *Semicond. Sci. Technol.* **19** R59
[11] Nishii J, Hossain F M, Takagi S, Aita T, Saikusa K, Ohmaki Y, Ohkubo I, Kishimoto S, Ohtomo A, Fukumura T, Matsukura F, Ohno Y, Koinuma H, Ohno H and Kawasaki M 2003 *Jpn. J. Appl. Phys.* **42** L347
[12] Hossain F M, Nishii J, Takagi S, Sugihara T, Ohtomo A, Fukumura T, Koinuma H, Ohno H and Kawasaki M 2004 *Physica* E **21** 911
[13] Norris B J, Anderson J, Wager J F and Kszler D A 2003 *J. Phys.* D: *Appl. Phys.* **36** L105
[14] Yang P, Yan H, Mao S, Russo R, Johnson J, Saykally R, Morris N, Pham J, He R and Choi H J 2002 *Adv. Mater.* **12** 323
[15] Ito Y, Kushida K, Sugawara K and Takeuchi H 1995 *IEEE Trans. Ultrasonics Ferroelectrics and Frequency Control* **42** 316
[16] Ryu H W, Park B S, Akbar S A, Lee W S, Hong K J, Seo Y J, Shin D C, Park J S and Choi G P 2003 *Sensor Actuator* B **96** 717
[17] Sberveglieri G 1995 *Sensor Actuator* B **23** 103
[18] Trivikrama Rao G S and Tarakarama Rao D 1999 *Sensor Actuator* B **55** 166
[19] Cheng X L, Zhao H, Huo L H, Gao S and Zhao J G 2004 *Sensor Actuator* B **102** 248
[20] Dietl T 2002 *Semicond. Sci. Technol.* **17** 377
[21] Sharma P, Gupta A, Rao K V, Owens F J, Sharma R, Ahuja R, Osorio J M, Johansson B and Gehring G A 2003 *Nat. Mater.* **2** 673
[22] Li C, Guo W, Kong Y and Gao H 2007 *Appl. Phys. Lett.* **90** 033108
[23] Vosko S H, Wilk L and Nusair M 1980 *Can. J. Phys.* **58** 1200
[24] Akai H and Dederichs P H 1993 *Phys. Rev.* B **47** 8739
[25] Akai H 1998 *Phys. Rev. Lett.* **81** 3002
[26] Salmani E, Benyoussef A, Ez-Zahraouy H and Saidi E H 2011 *Chin. Phys.* B **20** 086601
[27] MACHIKANEYAMA2002v09: Akai H, Department of Physics, Graduate School of Science, Osaka University, Machikaneyama 1-1, Toyonaka 560-0043, Japan, akai@phys.sci.osaka-u.ac.jp
[28] Balcerzak T 2004 *J. Magn. Magn. Mater.* **320** 272–276, 1035
[29] Balcerzak T 2003 *Physica* A **317** 213
[30] Jalbout A F, Chen H and Whittenburg S L 2002 *Appl. Phys. Lett.* **81** 2217
[31] Demokritov S O, Wolf J A and Grünberg P 1993 *J. Magn. Magn. Mater.* **126** 386
[32] Grünberg P 2001 *J. Magn. Magn. Mater* **226–230** 1688
[33] Bruno P and Chappert C 1992 *Phys. Rev.* B **46** 261
[34] Mounkachi O, Benyoussef A, El Kenz A, Saidi E H and Hlil E K 2008 *J. Magn. Magn. Mater.* **320** 2760
[35] Dietl T, Haury A and dAubigné Y M 1997 *Phys. Rev.* B **55** R3347
[36] Priour D J Jr, Hwang E H and Das Sarma S 2004 *Phys. Rev. Lett.* **92** 117201
[37] Mounkachi O, Benyoussef A, El Kenz A, Saidi E H and Hlil E K 2009 *Physica* A **388** 3433
[38] Joseph M, Tabata H and Kawai T 1999 *Jpn. J. Appl. Phys.* **38** L1205
[39] Sharma P, Gupta A, Rao K V, Owens F J, Sharma R, Ahuja R, Guillen J M O, Johansson B and Gehring G A 2003 *Nat. Mater.* **2** 673
[40] Tiwari A, Jin C, Kvit A, Kumar D, Muth J F and Narayan J 2002 *Solid State Commun.* **121** 371
[41] Lawes G, Ramirez A P, Risbud A S and Seshadri Ram 2005 *Phys. Rev.* B **71** 045201
[42] Cheng X M and Chien C L 2003 *J. Appl. Phys.* **93** 7876
[43] Jin Z, Yoo Y Z, Sekiguchi T, Chikyow T, Ofuchi H, Fujioka H, Oshima M and Koinuma H 2003 *Appl. Phys. Lett.* **83** 39
[44] Sato K and Katayama–Yoshida H 2001 *Jpn. J. Appl. Phys.* **40** L485
[45] Xu Q, Schmidt H, Hartmann L, Hochmuth H, Lorenz M, Setzer A, Esquinazi P, Meinecke C and Grundmann M 2007 *Appl. Phys. Lett.* **91** 092503